

Cluster-like resistive switching of SrTiO₃:Nb surface layers

This content has been downloaded from IOPscience. Please scroll down to see the full text.

2013 New J. Phys. 15 103017

(<http://iopscience.iop.org/1367-2630/15/10/103017>)

View [the table of contents for this issue](#), or go to the [journal homepage](#) for more

Download details:

IP Address: 134.94.122.141

This content was downloaded on 15/11/2013 at 13:24

Please note that [terms and conditions apply](#).

Cluster-like resistive switching of SrTiO₃:Nb surface layers

**C Rodenbücher^{1,2,7}, W Speier², G Bihlmayer^{1,2,3}, U Breuer⁴,
R Waser^{1,2,5} and K Szot^{1,2,6}**

¹ Forschungszentrum Jülich GmbH, Peter Grünberg Institut (PGI-7),
D-52425 Jülich, Germany

² Forschungszentrum Jülich GmbH, JARA—Fundamentals of Future
Information Technologies, D-52425 Jülich, Germany

³ Forschungszentrum Jülich, Institute of Advanced Simulation (IAS-1),
D-52425 Jülich, Germany

⁴ Forschungszentrum Jülich GmbH, Zentralinstitut für Engineering,
Elektronik und Analytik (ZEA-3), D-52425 Jülich, Germany

⁵ RWTH Aachen, Institut für Werkstoffe der Elektrotechnik 2,
D-52056 Aachen, Germany

⁶ University of Silesia, August Chełkowski Institute of Physics,
40-007 Katowice, Poland

E-mail: c.rodenbuecher@fz-juelich.de

New Journal of Physics **15** (2013) 103017 (14pp)

Received 28 June 2013

Published 17 October 2013

Online at <http://www.njp.org/>

doi:10.1088/1367-2630/15/10/103017

Abstract. The understanding of the resistive switching mechanisms in perovskites is of particular importance for the development of novel non-volatile memories. Nanoscale investigations recently revealed that in the model material SrTiO₃ a filamentary type of switching is present. In this paper, we show that upon donor doping with Nb the switching type changes fundamentally. We report on the observation of conducting clusters that can be switched independently between a high resistance and a low resistance state when applying a voltage. Furthermore, we show that the resistive switching takes place in a semiconducting surface layer on top of the metallic bulk of SrTiO₃:Nb single crystals, which can change its properties easily under external gradients.

⁷ Author to whom any correspondence should be addressed.



Content from this work may be used under the terms of the [Creative Commons Attribution 3.0 licence](http://creativecommons.org/licenses/by/3.0/). Any further distribution of this work must maintain attribution to the author(s) and the title of the work, journal citation and DOI.

Based on various measurements, we postulate that ionic movements leading to the creation of secondary phases as nano-filaments between the clusters have to be taken into account in modelling the resistive switching.

S Online supplementary data available from stacks.iop.org/NJP/15/103017/mmedia

Contents

| | |
|--|-----------|
| 1. Introduction | 2 |
| 2. Methods | 3 |
| 3. Results | 4 |
| 3.1. Resistive switching on the macroscale | 4 |
| 3.2. Resistive switching on the nanoscale | 6 |
| 3.3. Surface layer | 9 |
| 4. Discussion and conclusions | 11 |
| Acknowledgments | 13 |
| References | 13 |

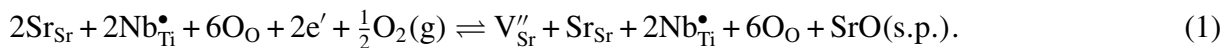
1. Introduction

In recent years SrTiO₃, a prototype perovskite material, has attracted much attention because it is possible to change its resistance from insulator to metal and even to superconductor [1] by applying electric fields thus making such materials very promising for future applications in redox-based resistive switching memory cells (ReRAM) [2]. Resistive switching has been reported in SrTiO₃ thin films [3] as well as in single crystals [4]. The switching between insulator and metal is related to the transition of a titanium ‘d’-electron from d⁰ to d² and d³. This ‘d’-electron can be generated either

- by a chemical gradient (reduction in low p_{O_2}),
- by an electrical gradient (electroreduction),
- by a convolution of these gradients,
- by donor doping.

Here, pentavalent Nb is used as a donor for SrTiO₃ substituting the tetravalent Ti. Although after this doping the crystal should be metallic at low carrier concentrations [5, 6], surprisingly, resistive switching can be observed in Nb-doped SrTiO₃ thin films [7] and even in single crystals [8–26], although the nature of the switching process is still under discussion (for details see supplement). Furthermore, a highly resistive surface layer, which arises as soon as the crystal comes into contact with oxygen, was detected on SrTiO₃:Nb influencing the properties of the whole sample [27, 28]. In general, it is well known that such surface layers exist in perovskites and they have been investigated intensively for BaTiO₃ [29, 30]. In our previous study on SrTiO₃:Nb thin films [7], we showed that the resistive switching on the nanoscale is not of a filamentary type, as in undoped SrTiO₃, but is related to the presence of regularly arranged switching blocks representing a cluster-like switching behaviour. In the present paper, we intend to focus on the fundamental physical mechanisms behind

this behaviour by investigating the properties of Nb-doped single crystals on the macro- and the nanoscale. In order to obtain an insight into the origin of the resistive switching phenomenon in single crystals, a careful investigation of the local structure and chemical composition of surface layer and bulk has to be made since in SrTiO₃ clustering of defects as found in doped and undoped thin films [7, 31, 32] or a formation of secondary phases can easily evolve. According to the redox equation, which describes the defect chemistry of the Nb doping, the donor compensation can change under oxidizing conditions from electronic compensation to compensation by Sr vacancies leading to the creation of SrO, which can form Ruddlesden–Popper phases or islands on the surface [33–36]. Simultaneously, the sample changes from a metal to a highly insulating material



Here, the Kröger–Vink notation is used and the equation is expressed for two units of the ABO₃ perovskite crystal. (g) and (s.p.) denote the gas phase and a secondary solid phase, respectively. Due to the frozen-in Schottky equilibrium, the oxygen vacancy concentration in donor-doped SrTiO₃ is extremely low. If the chemical composition deviates from the stoichiometric case, which may occur for inhomogeneities of the surface layer, different reactions will take place. In Sr-deficient SrTiO₃, reduction leads to the creation of Ti-rich phases [36], which have been found particularly in doped SrTiO₃ [37–41]. Further reduction of TiO₂ can then lead to the formation of substoichiometric titanium oxides such as Magnéli phases [42]:



In this paper, we investigate the resistive switching related to the transport behaviour on the macroscale by electrical four-point measurements and on the nanoscale by local conductivity atomic force microscopy (LC-AFM) under ultra-high vacuum (UHV) conditions. Based on careful investigations of the surface layer under chemical and electrical gradients, we suggest a nanoscale model of the resistive switching.

2. Methods

The present measurements were conducted on commercially available epi-polished SrTiO₃:Nb (100) single crystals with a doping concentration of 1.4 at.% supplied by Crystec (Berlin) and Mateck (Jülich). X-ray diffraction measurements were performed using an STOE instrument on powders of the single crystals with a doping concentration of 0.2, 1.4 and 10.1 at.%, and the lattice constant was determined using Rietveld refinement. Additionally, a Si standard (NIST 640c) was added to take zero shift into account. Electrical measurements on the macroscale were performed using a home-made probe station on samples contacted with Pt paste under ambient conditions. For the four-point measurements in Valdes geometry, Pt electrodes were sputtered on the epi-polished side of the sample. Under UHV conditions, a voltage was applied to two electrodes and the potential between all four electrodes was measured by electrometers. To carry out temperature-dependent four-point measurements up to a temperature of 1000 °C, Pt electrodes were pasted in the same geometry as the sputtered ones. Etching of the sample was performed using hydrofluoric acid to obtain etch pits at the exits of the dislocations on the surface. LC-AFM measurements were made using a JEOL JSPM setup with a Pt/Ir-coated silicon tip in contact mode under vacuum conditions and at different temperatures. During the scan, a bias voltage of 5–10 mV was applied to the tip and the measured current was used

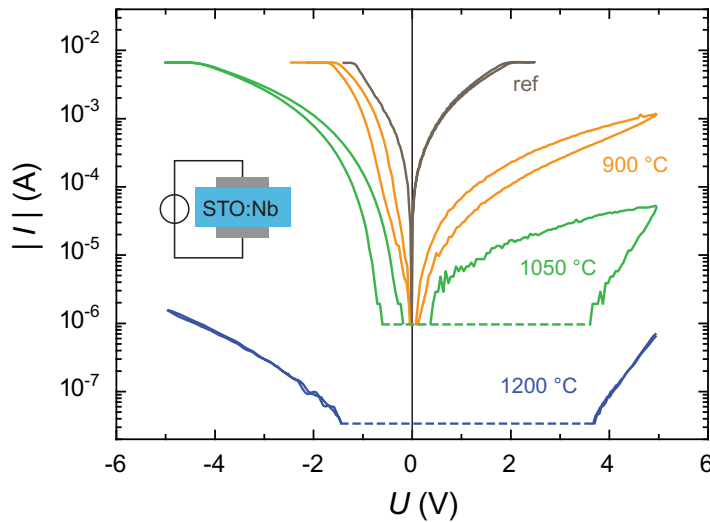


Figure 1. Resistive switching on the macroscale. I – V curves obtained at samples oxidized at different temperatures. (The dotted lines indicate the respective noise level.)

to calculate the resistance of the sample after subtraction of the noise level using Gwyddion software [43]. X-ray photoelectron spectroscopy (XPS) spectra were obtained by a Perkin-Elmer instrument using monochromatized Al- K_{α} rays under UHV conditions. The background of the spectra was subtracted by the Shirley method and the peaks were simulated by Gauss–Lorentz functions. Atom probe measurements were conducted on a CAMECA LEAP4000 X HR instrument using UV-laser pulsing after preparing a small needle of SrTiO₃:Nb (1.4 at.%) by a focused ion beam. Finite element simulations were conducted using an ANSYS program simulating clusters with a diameter of 40 nm. The assumed values for the resistivity were $\rho_c = 1 \times 10^{-6} \Omega \text{ m}$ for the clusters and $\rho_m = 1 \times 10^2 \Omega \text{ m}$ for the matrix according to the simulations for homogeneous SrTiO₃ thin films [44]. The resistivity of the bridge was adjusted to $\rho_b = 1.3 \times 10^{-2} \Omega \text{ m}$ corresponding to our measurements where a switching voltage of 4 V results in a current of 1 μA . For the thermal conductivity k , temperature-dependent values were chosen on the basis of laser flash measurements. At room temperature the thermal conductivity is $k = 9 \text{ W m}^{-1} \text{ K}^{-1}$ and at higher temperatures it decreases according to a $1/T$ law.

3. Results

3.1. Resistive switching on the macroscale

The resistive switching behaviour was investigated by performing electrical measurements on the macroscale. Three unpolished samples ($5 \times 5 \times 0.5 \text{ mm}$) cut from the same crystal were investigated after annealing in air for 5 h at different temperatures. Additionally, one as-received reference sample was measured. The samples were contacted using Pt paste on the top and the bottom side, and I – V curves were measured as shown in figure 1. It can be seen that the conductivity decreases systematically upon increasing the annealing temperature. Furthermore, all samples besides that annealed at 1200 °C exhibited bipolar resistive switching, which is surprising since the geometry of samples and electrodes was nominally symmetrical.

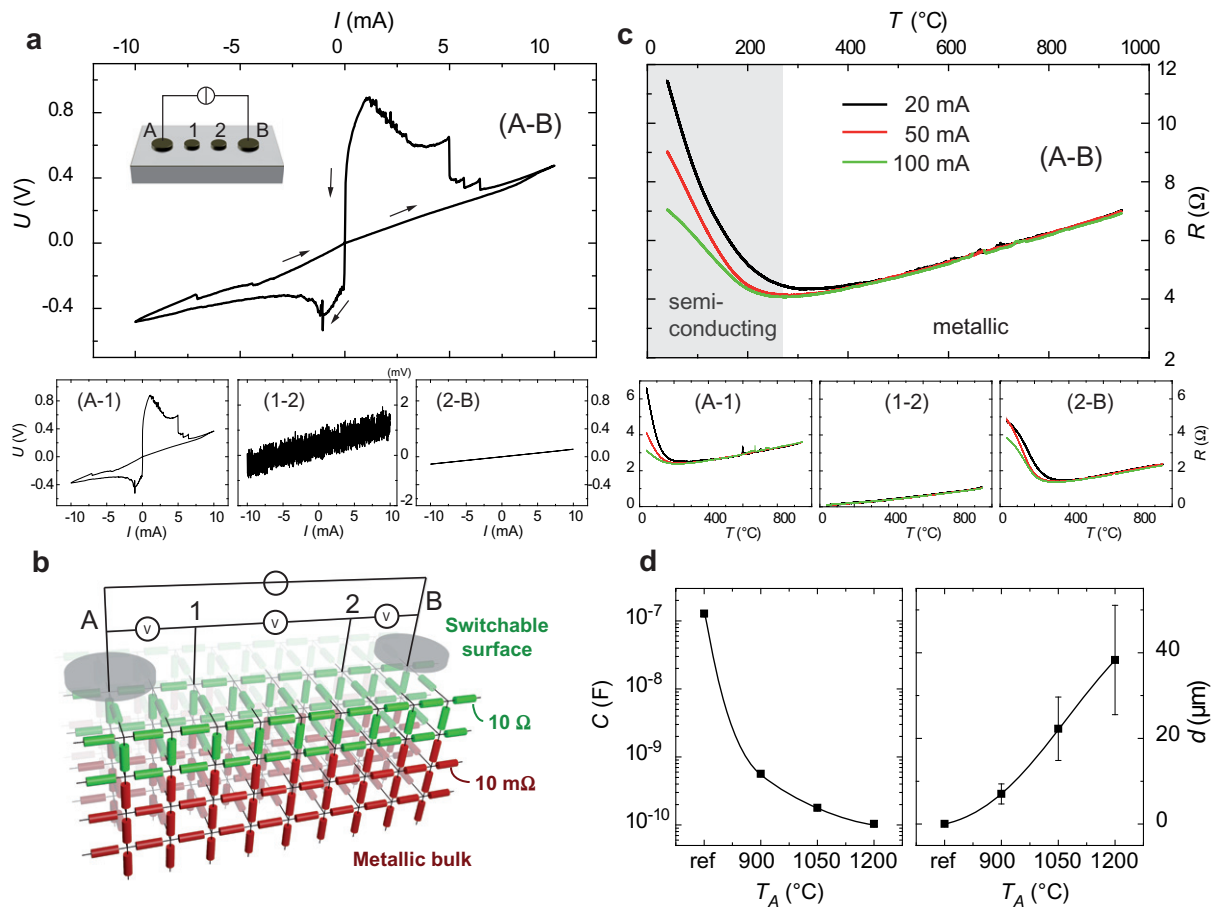


Figure 2. Electrical measurement of the surface layer. (a) $V-I$ curve obtained under UHV conditions between outer electrodes showing switching behaviour. Below: voltage between the inner and outer electrodes. (b) Simulation of the resistance of the sample by a network of resistors representing surface layer (green) and bulk (red). (c) Resistance as a function of temperature after electroreduction with different currents. (d) Capacitance and calculated thickness of the surface layer measured on samples oxidized at different temperatures.

This indicates that an asymmetry was introduced in the system related to the preparation procedure or to electroforming effects. In order to investigate the effect of electrodegradation on the surface layer, which could be the reason for the appearance of bipolar switching, we conducted four-point measurements in Valdes geometry (cf figure 2). The outer electrodes were connected to a current source and the potential between the outer and inner electrodes was measured. The $V-I$ curves recorded between electrodes A and B displayed occasional bipolar switching behaviour as shown in figure 2(a). Regarding the individual contributions between the inner electrodes, we can see that switching only occurred between electrodes A and 1. Although the electrodes were symmetrical, electrode A had the role of the anode at the beginning of the voltage sweep and the asymmetry could have been created by ionic movements, as will be discussed below. The potential between the inner electrodes 1 and 2, representing the properties of the bulk, showed ohmic behaviour with low resistance confirming

that not the bulk of the sample but only the surface layer is responsible for the switching. To illustrate the difference between bulk and surface, we performed a simulation program with integrated circuit emphasis (SPICE) simulation as depicted schematically in figure 2(b). We assumed a network of resistors with two rows ($10\ \Omega$ each) representing the highly resistive surface layer while the resistors representing the bulk had much lower resistances of $10\ \text{m}\Omega$. The simulation qualitatively reproduced the ratio of the measured voltages between the inner and outer electrodes and proved that the assumption of a surface layer with high resistivity was justified. The difference between the bulk and the surface layer becomes even more obvious with temperature-dependent measurements. While the as-received surface layer was semiconducting with a high resistance ($>10^8\ \Omega$), the resistance dropped significantly after performing electroreduction by applying a constant current to the outer electrodes at $1000\ ^\circ\text{C}$. The resistance curves measured during cooling (figure 2(c)) showed a characteristic and reproducible temperature dependence. Starting at high temperature, at first the resistance decreased with the decreasing temperature indicating metallic behaviour until a minimum was reached around $250\ ^\circ\text{C}$. Upon further cooling, the resistance increased again indicating semiconducting behaviour. If more powerful electroreduction was performed by increasing the current, the shapes of the curves at higher temperatures did not change at all, whereas the resistance of the semiconducting part was reduced. In contrast to the surface layer, the bulk had metallic properties throughout the whole temperature range as expected for doped SrTiO_3 . In order to estimate the thickness of the surface layer, we measured the serial capacitance using a small ac voltage ($100\ \text{mV}$, $10\ \text{kHz}$) on the same samples as investigated in figure 1. We obtained a very high capacitance, which decreases with the annealing temperature T_A (figure 2(d)). The high value of the capacitance indicates that not the whole volume of the sample but only the surface layers contribute to the measured capacitance. This gives us the opportunity to estimate the thickness of the surface layer. Therefore we assumed the relative permittivity to be $\epsilon = 300$, which is a typical value of SrTiO_3 , and we calculated the thickness. While the thickness of the surface layer of the as-received sample was only in the range of $30\ \text{nm}$, the thickness increased to $40\ \mu\text{m}$ after annealing under oxidizing conditions.

In conclusion, the electrical measurements provide evidence of the existence of a highly resistive surface layer on top of the as-received crystal being responsible for the resistive switching.

3.2. Resistive switching on the nanoscale

Having seen that the resistive switching is related to the surface layer, we now proceed to investigate the spatial homogeneity of the resistivity of the surface layer. Therefore, we conducted a typical LC-AFM switching experiment on the as-received sample ($1.4\ \text{at.}\% \text{Nb}$) under HV conditions at $50\ ^\circ\text{C}$. First a region of $500\ \text{nm} \times 500\ \text{nm}$ was scanned while a switching voltage of $+4\ \text{V}$ was permanently applied. After this, the same area was scanned again with a reading voltage of $10\ \text{mV}$. The result is shown in figure 3(a). It can be seen that the whole scanned area has switched to the ON state with a significantly smaller resistance than the untreated surface. Furthermore, it can be seen that the conductivity of the switched area is not homogeneous but shows an array of conducting clusters with an average diameter of around $50\ \text{nm}$. The clusters are regularly aligned in rows oriented along the $\langle 100 \rangle$ crystal axes, which is not an artefact of the scan procedure since this was excluded by switching scans under different angles between tip movement and sample orientation. In order to further demonstrate that the cluster-like switching behaviour is a property of the Nb-doped crystal itself,

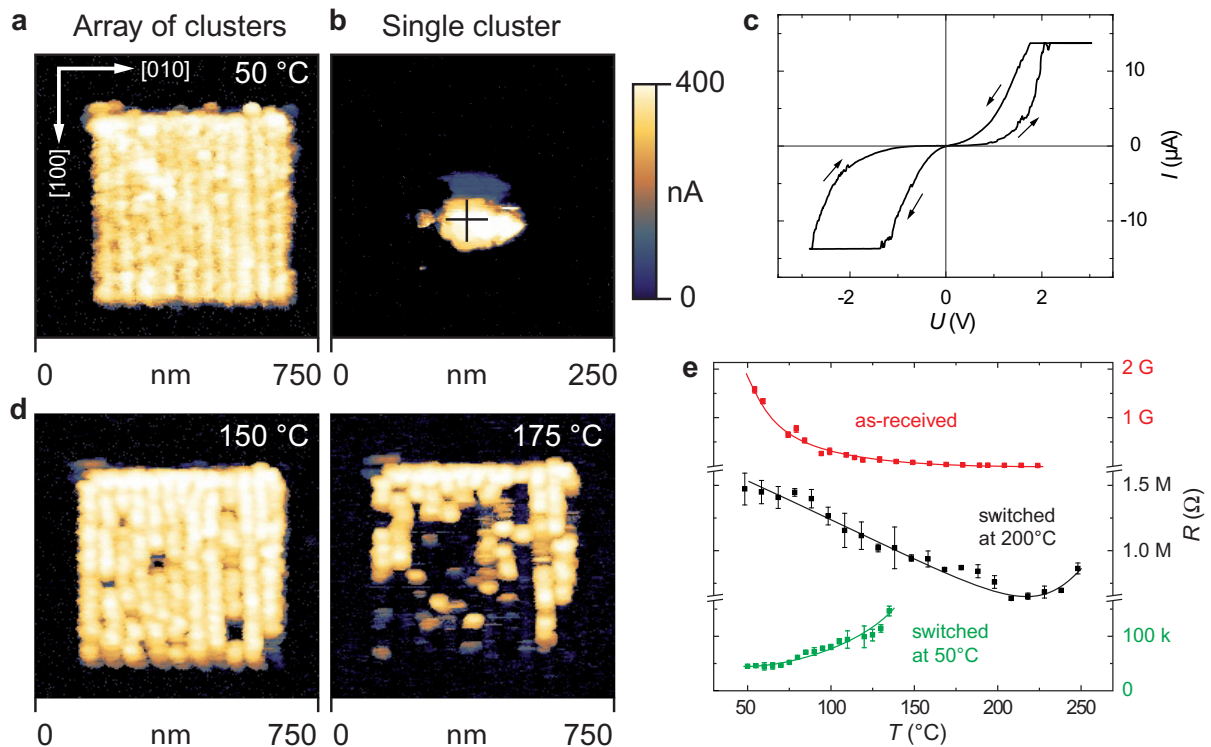


Figure 3. Resistive switching on the nanoscale. (a) LC-AFM images showing the switching of an array of clusters by performing a continuous switching scan and (b) the switching of a single cluster by the application of the switching voltage (+4 V) in one point at 50 °C. (c) Local I - V characteristic during switching. (d) Back-switching of the array of clusters at higher temperatures. (e) Resistance as a function of temperature calculated from LC-AFM scans for the as-received surface and the ON states obtained by switching at 200 and 50 °C.

we attempted to switch one single point (marked by a cross in figure 3(b)) by applying the switching voltage (+4 V) without moving the AFM tip. After this, not only the contact point but the whole cluster switched to the ON state proving that the nanoscale resistive switching is not of a filamentary type, as in undoped SrTiO₃, but reveals a cluster-like dimension. The local I - V curve (figure 3(c)) measured at one point of the surface shows that the resistance could be switched between two resistance states by electrical gradients comparable to the macroscopic measurements. The switching polarity corresponds to the so-called ‘eightwise’ switching [45] and is in agreement with the switching scans conducted on Nb-doped thin films [7]. To check the stability of the ON state of the clusters, we increased the temperature and obtained measurements of the switched array (figure 3(d)). Below 150 °C the conductivity did not change at all, but at higher temperatures the clusters started to switch back. It can be seen that the clusters always switched back as a whole and independently of each other. At 175 °C most of the clusters finally switched back after some time. The switching of the clusters by electrical gradients on the nanoscale is related to an insulator-to-metal transition, which is proved by the calculations of the resistance extracted from LC-AFM measurements at different temperatures (figure 3(e)). The as-received surface had a very high resistance, which

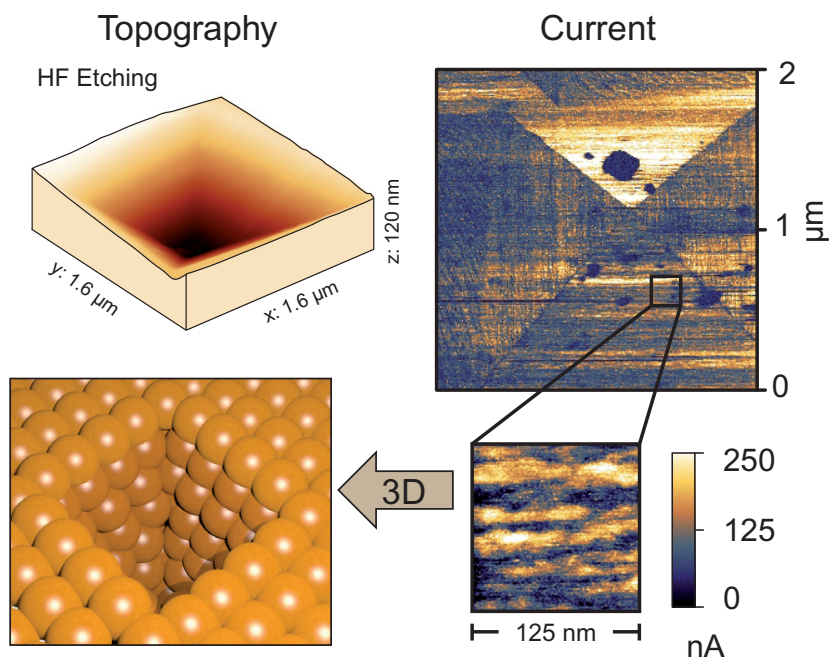


Figure 4. Investigations of clusters. Topography and current measured by LC-AFM in an etch-pit showing the presence of three-dimensional (3D) clusters in the bulk.

clearly showed a semiconducting behaviour. After switching at 200 °C, the resistivity of the clusters is in a lower resistance state. The temperature dependence of the resistance shows a minimum resistance at approximately 225 °C comparable to the temperature dependence obtained by the macroscopic measurement in figure 2(c). In contrast, the third graph, obtained after switching at 50 °C from the measurement in figure 3(b), shows a metallic behaviour up to 150 °C. At higher temperatures, these clusters switched back to the OFF state probably due to re-oxidation effects (cf supplementary figure S3 and supplementary video 1, available from stacks.iop.org/NJP/15/103017/mmedia). The different behaviour of the resistivity depending on the conditions during switching indicates that the surface layer is highly variable under the applied gradients.

In the next section we will examine the nature of the conducting clusters. In order to check whether these clusters are only related to the surface layer or also exist in the bulk, we etched the crystal for 10 min in buffered hydrofluoric acid (12.5% HF) at 90 °C. During this procedure, etch pits evolved from the surface providing a ‘tomographic view’ into the bulk of the sample. As shown in figure 4(a), the conductivity measured in one etch pit shows a conductivity pattern with clusters, which indicates that the clusters are present everywhere in the crystal. The clusters are aligned in rows at the sides of the etch pit revealing a long-range order in the conductivity. Such a long-range order in the related density of states was previously found in Nb-doped SrTiO₃ as measured by scanning tunnelling microscopy on cleaved crystals [46].

Summarizing the investigations on the nanoscale by means of LC-AFM, we found regularly arranged conducting clusters that could be switched independently between the ON and OFF state. In contrast to the filamentary switching in undoped SrTiO₃, in Nb-doped SrTiO₃ a different cluster-like switching mechanism is present.

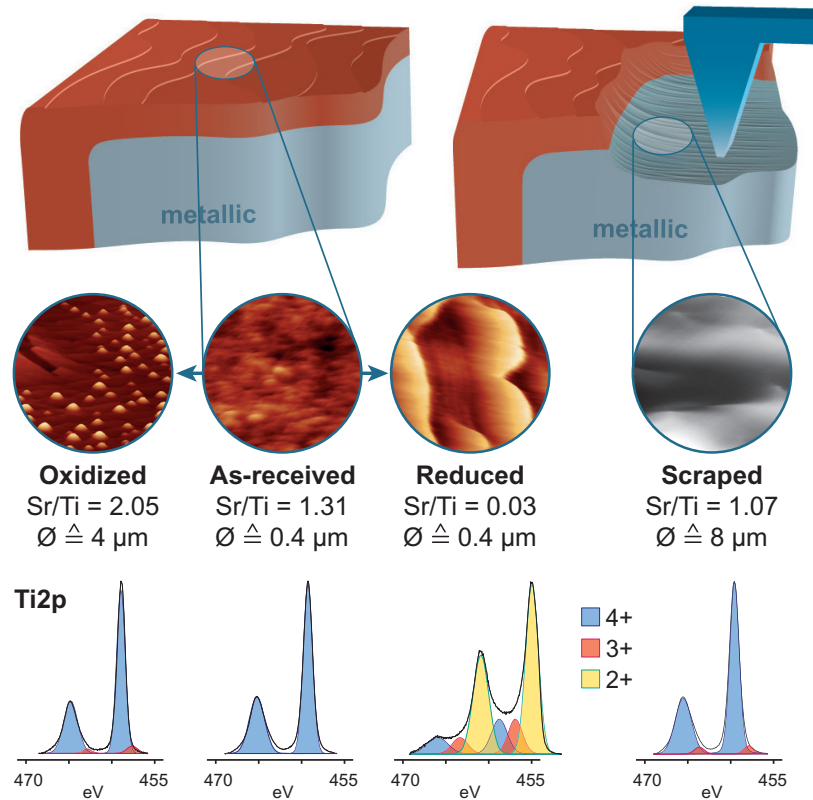


Figure 5. Investigation of the surface layer. Illustration of a cross section through the sample before and after removing the surface layer by scraping with the corresponding AFM topography images and Sr/Ti ratios and Ti 2p valences obtained by XPS after application of different gradients.

3.3. Surface layer

Having seen that the surface layer of the crystal is responsible for the resistive switching phenomena, we now want to focus on the fundamental physical properties of this layer. By XPS measurements of the as-received surface we found an excess of Sr and no metallic states at the Fermi edge, which is in agreement with the conclusions derived from the electrical measurements. However, by removing the surface *in situ* under UHV conditions by scraping with a diamond tip (figure 5), we obtained access to the bulk properties and we found a perfect stoichiometry with a Sr/Ti ratio close to 1 and we were able to measure indications of metallic states at the Fermi edge in the electronic structure, which is consistent with the results on cleaved samples obtained by Haruyama *et al* [28]. We can thus conclude that the samples were grown with a perfect stoichiometry but that a surface layer with properties different than the bulk has evolved in air. Regarding the shape of the Ti 2p core line after scraping, we can detect a contribution of the valence state +3, indicating that Nb doping is not mainly compensated by the creation of cation vacancies but by a change of the Ti valences, which can be expressed by the structural formula $\text{SrTi}_{1-x}^{4+}\text{Ti}_x^{3+}\text{Nb}_x^{5+}\text{O}_3$. The stoichiometry of the surface layer can be altered dramatically by different treatments (see also supplementary figure S8, available from stacks.iop.org/NJP/15/103017/mmedia). If the surface is reduced

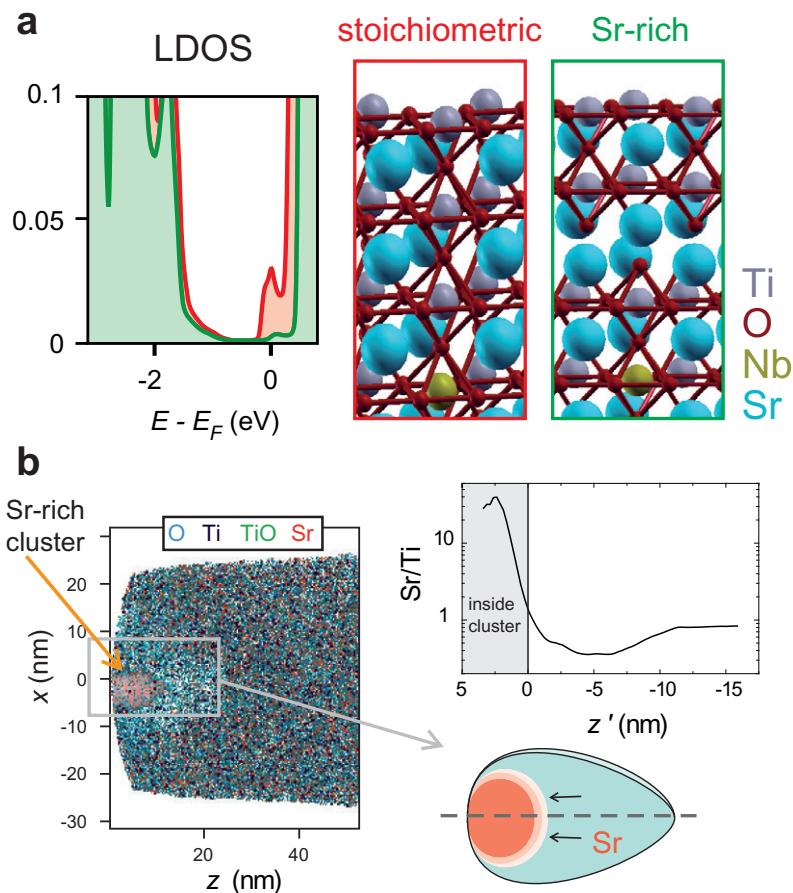


Figure 6. Sr-rich surface layer (a) LDOS simulations of a stoichiometric and Sr-rich surface. (b) Atom probe measurement of Sr-movement induced by FIB.

by heating for 24 h at 1100 °C under UHV conditions, only a small amount of Sr is left in the surface layer. Simultaneously, the electronic structure changes considerably with Ti and Nb mainly displaying valence +2, which is consistent with our previous findings [47]. This indicates that reduction can form Ti-rich phases at the surface. Effusion measurements during reduction revealed that no Sr-related components are emitted from the sample indicating that Sr diffuses into the bulk of the crystal. Heating the sample under oxidizing conditions instead increases the amount of Sr and no additional valences are visible thus indicating the formation of Sr-rich micro crystals on the surface, as predicted by formula (1) and also proved by previous measurements [48, 49]. In order to understand the differences between the Sr-rich as-received surface layer and the stoichiometric bulk, we performed *ab initio* calculations of Nb-doped SrTiO₃ in two different structural models (for details see supplementary figure S9, available from stacks.iop.org/NJP/15/103017/mmedia), which revealed that metallic states at the Fermi edge are suppressed by an excess of Sr modelled by Ruddlesden–Popper layers (figure 6(a)). This corresponds to the electrical measurements in figure 1 where we showed that annealing under oxidizing conditions increases the thickness and the Sr content of the surface layer and simultaneously suppresses the conductivity. In order to reconstruct the metallic properties of the surface layer, which would be the decisive step in the

resistive switching process, a Sr movement has to take place. To illustrate the possibility of Sr movements under external gradients, we performed measurements using a 3D atom probe (figures 6(b) and S10, available from stacks.iop.org/NJP/15/103017/mmedia). A sharp needle was cut out of the SrTiO₃:Nb by a focused ion beam resulting in the formation of a Sr-rich cluster at the end of the needle associated with the evolution of a Ti-rich region below. This measurement confirms the possibility of Sr movements, which have also been reported in relation to the formation of Ruddlesden–Popper phases under electrical [50] and thermal [51] gradients, as well as in relation to the segregation of SrO [48]. In general, we can conclude that the chemical composition of the surface layer is highly variable under chemical gradients and in particular Sr-rich or Ti-rich phases can be formed, which we have to bear in mind when establishing a nanoscale model of resistive switching in the following.

4. Discussion and conclusions

Summarizing the results presented, we first of all found that the resistive switching is related to conducting clusters. Hence, the switching mechanism in Nb-doped SrTiO₃ differs from the switching of extended filaments in undoped SrTiO₃. Furthermore, we demonstrated by LC-AFM measurements that resistive switching is possible without a permanent electrode indicating that fundamental changes take place during switching in the surface layer. Since the conducting clusters are present in Nb-doped SrTiO₃ and exhibit higher conductivity than the surrounding matrix, one possible explanation for the evolution of the clusters could be that the Nb content inside these clusters is slightly higher than in the surrounding matrix. Although the XRD measurements (supplementary figure S1) suggest that on average most of the Nb is distributed homogeneously, small fluctuations on the nanoscale could be responsible for the formation of the clusters. As demonstrated by density functional theory calculation (supplementary figure S7), such a Nb clustering could be possible in principle. This is supported by the fact that we were able to detect Nb segregation effects on the macroscale in the outer shell of several crystals related to the crystal growth process (supplementary figure S6). Using an atom probe we demonstrated that due to ion beam irradiation not only the ratio of Sr and Ti but also the Nb content can be changed illustrating the possibility of Nb segregation on the nanoscale (supplementary figure S10). A further indication of the possibility of Nb clustering is that such donor clustering has been shown for Ba-doped SrTiO₃ by calculations [52] and experiments [53], and the existence of Nb clusters was also proposed [31] for Nb-doped SrTiO₃ thin films. An alternative explanation for the evolution of the clusters could be that an agglomeration of Sr vacancies leading to a small local distortion of the lattice takes place, which was proposed earlier for non-stoichiometric SrTiO₃ as well as for Nb-doped thin films [7, 32].

In order to model the resistive switching, not only the presence of clusters but also the existence of the semiconducting surface, which was found on top of the metallic bulk, has to be taken into account. Especially the ability to form Ti-rich or Sr-rich phases under applied gradients such as reduction and oxidation is highly relevant since the application of electric fields during the resistive switching leads to the presence of comparable gradients on the nanoscale. Since the bulk was found to be fully metallic, resistive switching can only take in the surface layer. Based on the observation that the conducting clusters can always be switched as a whole and independently of each other, we assume that not the clusters themselves but rather the contact regions between the clusters, which we call bridges, are switching. Hence, we

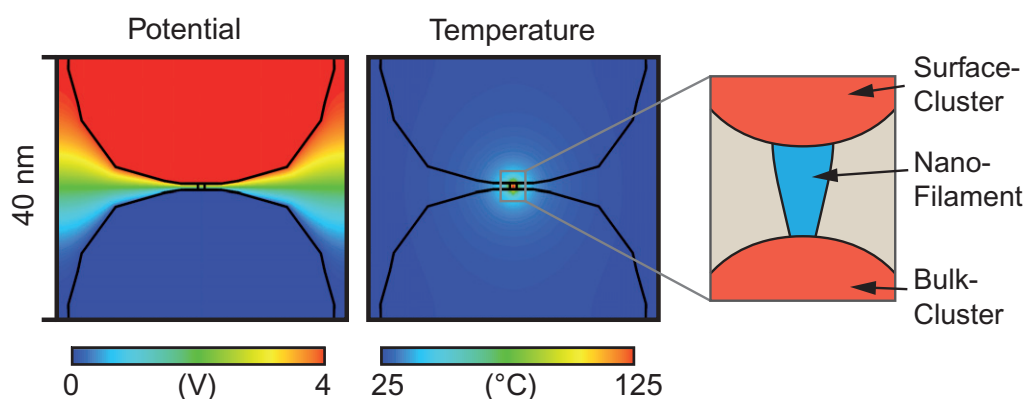


Figure 7. Model of the electroformation and the resistive switching of Ti-rich nano-filaments between conducting clusters.

propose the following two-step model of resistive switching. While the clusters and bridges of the bulk are always in the metallic state and are not affected by the switching process, the topmost clusters, which build up the semiconducting Sr-rich surface layer, have to be transformed to metallic clusters with perfect stoichiometry related to Sr/SrO movement via a first electroforming process by applying a positive voltage to the AFM tip. When the clusters are in the metallic state, the greatest drop in potential occurs in the region between the clusters displaying higher resistivity. We simulated this situation by a finite element method, as shown in figure 7, by calculating the potential and temperature during switching. It was assumed that two conducting clusters are connected by a bridge with higher resistivity. The simulation reveals that in this case the entire potential drops in the region between the clusters, which in the model was only a few nanometres in size. This leads to the presence of high electric fields, although the temperature only increases slightly indicating that thermal effects play a minor role during the switching process. Hence we assume that ionic movements take place caused by electric gradients. Since we have seen that Sr/SrO is highly mobile under applied gradients, we conclude that the high electric field in the region between the clusters leads to the formation of a Ti-rich bridge, probably consisting of one or several Ti_nO_{2n-1} phases. Once such a bridge, which can be regarded as a nano-filament, is formed, the resistive switching can be explained by taking into account oxygen movements switching the bridge from a highly conducting Ti_nO_{2n-1} phase to a poorly conducting phase and vice versa, depending on the polarity of the applied voltage. In comparison to undoped $SrTiO_3$, in which filaments related to extended defects were found to be responsible for the switching, Nb doping leads to the presence of clusters either directly by Nb clustering or indirectly by the formation of clustering vacancies as described above. This suppresses the switching mechanism along the extended defects and confines the switching to a region between the topmost conducting clusters in the surface layer, where a nano-filament is formed. According to this description, the Nb itself only plays a minor role during the switching process.

The existence of such titanium oxide phases would also explain the characteristic temperature-dependent resistance curves measured after electrodegradation on the macro- and the nanoscale showing semiconducting behaviour up to 250 °C and metallic behaviour at higher temperatures (figures 2 and 3). On the one hand, this behaviour could be explained classically by a serial connection of the semiconducting contact resistance and the metallic bulk, but we

believe, especially because we found the same temperature dependence of the resistance on the macro- and on the nanoscale, that it represents a Mott transition between the insulator and metal. It is well known that such a transition occurs in Magnéli phases and especially that Ti_2O_3 undergoes a Mott transition between 200 and 300 °C [42], which leads us to conclude that this phase was created during the electrodegradation and then affected the resistance of the whole sample. Hence, we regard the measurement of the characteristic resistance curve as a strong indication of the formation of Ti-rich phases in $\text{SrTiO}_3:\text{Nb}$ under electrical gradients.

In summary, the resistive switching in the nominally metallic system $\text{SrTiO}_3:\text{Nb}$ can only be understood if the special role of the intrinsic Sr-rich semiconducting surface layer is considered. On the nanoscale, conducting and switchable clusters are present indicating that the switching mechanism in $\text{SrTiO}_3:\text{Nb}$ differs from the switching of extended filaments in undoped SrTiO_3 . We proposed a model suggesting that switching is a very complex local phenomenon related to the presence of conducting clusters and the generation of secondary phases as nanofilaments. Such a description is not limited to $\text{SrTiO}_3:\text{Nb}$ but may also be relevant for other oxides, in which a local filamentary switching mechanism is present.

Acknowledgments

We thank R Borowski, J Friedrich, M Gerst, M Grates, S Masberg and T Pössinger for technical support. Furthermore, we thank A Besmehn, M Ermrich and E Würtz for contributing measurements. Finally, we gratefully acknowledge J Mayer and P Meuffels for fruitful discussions. This work was supported in part by the Deutsche Forschungsgemeinschaft (SFB 917).

References

- [1] Schooley J F, Hosler W and Cohen M 1964 *Phys. Rev. Lett.* **12** 474–5
- [2] Beck A, Bednorz J G, Gerber C, Rossel C and Widmer D 2000 *Appl. Phys. Lett.* **77** 139–41
- [3] Oligschlaeger R, Waser R, Meyer R, Karthäuser S and Dittmann R 2006 *Appl. Phys. Lett.* **88** 042901
- [4] Szot K, Speier W, Bihlmayer G and Waser R 2006 *Nature Mater.* **5** 312–20
- [5] Tufte O N and Chapman P W 1967 *Phys. Rev.* **155** 796–802
- [6] Nakamura H, Takagi H, Inoue I H, Takahashi Y, Hasegawa T and Tokura Y 2006 *Appl. Phys. Lett.* **89** 133504
- [7] Münstermann R, Dittmann R, Szot K, Mi S, Jia C L, Meuffels P and Waser R 2008 *Appl. Phys. Lett.* **93** 023110
- [8] Sim H *et al* 2005 *IEDM Tech. Dig.* 777–80
- [9] Seong D J, Jo M, Lee D and Hwang H 2007 *Electrochem. Solid-State Lett.* **10** H168–70
- [10] Lee J *et al* 2010 *Curr. Appl. Phys.* **10** e68–70
- [11] Rana K G, Khikhlovskiy V and Banerjee T 2012 *Appl. Phys. Lett.* **100** 213502
- [12] Park C, Seo Y, Jung J and Kim D W 2008 *J. Appl. Phys.* **103** 054106
- [13] Shang D S, Sun J R, Shi L and Shen B G 2008 *Appl. Phys. Lett.* **93** 102106
- [14] Zhang X T, Yu Q X, Yao Y P and Li X G 2010 *Appl. Phys. Lett.* **97** 222117
- [15] Seong D J, Lee D, Pyun M, Yoon J and Hwang H 2008 *Japan. J. Appl. Phys. Part 2* **47** 8749–51
- [16] Kan D, Kan K and Shimakawa Y 2010 *Thin Solid Films* **518** 3246–49
- [17] Chen Y L, Wang J, Xiong C M, Dou R F, Yang J Y and Nie J C 2012 *J. Appl. Phys.* **112** 023703
- [18] Chen X G, Ma X B, Yang Y B, Chen L P, Xiong G C, Lian G J, Yang Y C and Yang J B 2011 *Appl. Phys. Lett.* **98** 122102
- [19] Gwon M, Lee E, Sohn A, Bourim E M and Kim D W 2010 *J. Korean Phys. Soc.* **57** 1432–6
- [20] Bourim E M and Kim D W 2013 *Curr. Appl. Phys.* **13** 505–9

- [21] Shen J X, Qian H Q, Wang G F, An Y H, Li P G, Zhang Y, Wang S L, Chen B Y and Tang W H 2013 *Appl. Phys. A* **111** 303–8
- [22] Zhong S and Cui Y 2013 *Curr. Appl. Phys.* **13** 913–8
- [23] Buzio R, Gerbi A, Gadaleta A, Anghinolfi L, Bisio F, Bellingeri E, Siri A S and Marrè D 2012 *Appl. Phys. Lett.* **101** 243505
- [24] Sun J, Jia C H, Li G Q and Zhang W F 2012 *Appl. Phys. Lett.* **101** 133506
- [25] Zhang P, Meng Y, Liu Z, Li D, Su T, Meng Q, Mao Q, Pan X, Chen D and Zhao H 2012 *J. Appl. Phys.* **111** 063702
- [26] Sawa A 2008 *Mater. Today* **11** 28–36
- [27] Han L Q, Kaimai A, Yashiro K, Nigara Y, Kawada T, Mizusaki J, Chen P, Zhong C and Higuchi T 2004 *Solid State Ion.* **175** 431–5
- [28] Haruyama Y, Aiura Y, Bando H, Suzuki H and Nishihara Y 1997 *Physica B* **237–8** 380–2
- [29] Känzig W 1955 *Phys. Rev.* **98** 549–50
- [30] Toyoda H and Itakura M 1962 *J. Phys. Soc. Japan* **17** 924–31
- [31] Zhu Y, Ma X, Li D, Lu H, Chen Z and Yang G 2005 *Acta Mater.* **53** 1277–84
- [32] Tokuda Y, Kobayashi S, Ohnishi T, Mizoguchi T and Shibata N 2011 *Appl. Phys. Lett.* **99** 033110
- [33] Akhtar M J, Akhtar Z, Jackson R A and Catlow C R 1995 *J. Am. Ceram. Soc.* **78** 421–8
- [34] Szot K, Speier W, Herion J and Freiburg C 1997 *Appl. Phys. A* **64** 55–9
- [35] Gunhold A, Gomann K, Beuermann L, Frerichs M, Borchardt G, Kempter V and Maus-Friedrichs W 2002 *Surf. Sci.* **507** 447–52
- [36] Blennow P, Hagen A, Hansen K K, Wallenberg L R and Mogensen M 2008 *Solid State Ion.* **179** 2047–58
- [37] Witek S, Smyth D M and Pickup H 1984 *J. Am. Ceram. Soc.* **67** 372–5
- [38] Fujimoto M and Watanabe M 1985 *J. Mater. Sci.* **20** 3683–90
- [39] Hung K and Yang W 2003 *Mater. Sci. Eng. A* **351** 70–80
- [40] Gunhold A, Beuermann L, Frerichs M, Kempter V, Gomann K, Borchardt G and Maus-Friedrichs W 2003 *Surf. Sci.* **523** 80–8
- [41] Kolodiaznyi T and Petric A 2005 *J. Electroceram.* **15** 5–11
- [42] Szot K, Rogala M, Speier W, Klusek Z, Besmehn A and Waser R 2011 *Nanotechnology* **22** 254001
- [43] Necas D and Klapetek P 2012 *Cent. Eur. J. Phys.* **10** 181–8
- [44] Menzel S, Waters M, Marchewka A, Böttger U, Dittmann R and Waser R 2011 *Adv. Funct. Mater.* **21** 4487–92
- [45] Muenstermann R, Menke T, Dittmann R and Waser R 2010 *Adv. Mat.* **22** 4819
- [46] Guisinger N P, Santos T S, Guest J R, Chien T Y, Bhattacharya A, Freeland J W and Bode M 2009 *ACS Nano* **3** 4132–6
- [47] Szot K and Speier W 1999 *Phys. Rev. B* **60** 5909–26
- [48] Szot K, Speier W, Breuer U, Meyer R, Szade J and Waser R 2000 *Surf. Sci.* **460** 112–28
- [49] Meyer R, Szot K and Waser R 1999 *Ferroelectrics* **224** 323–9
- [50] Meyer D, Levin A, Leisegang T, Gutmann E, Paufler P, Reibold M and Pompe W 2006 *Appl. Phys. A* **84** 31–5
- [51] Szot K, Pawelczyk M, Herion J, Freiburg C, Albers J, Waser R, Hulliger J, Kwapulinski J and Dec J 1996 *Appl. Phys. A* **62** 335–43
- [52] Fuks D, Dorfman S, Piskunov S and Kotomin E 2005 *Phys. Rev. B* **71** 14111
- [53] Rossell M D, Ramasse Q M, Findlay S D, Rechberger F, Erni R and Niederberger M 2012 *ACS Nano* **6** 7077–83